Quantum Storage of Single-Photon and Two-Photon Fock States with an All-Optical Quantum Memory

M. Bouillard, G. Boucher, J. Ferrer Ortas, B. Pointard, and R. Tualle-Brouri
Laboratoire Charles Fabry, Institut d'Optique Graduate School, CNRS, Université Paris-Saclay, 2 Avenue Augustin Fresnel, 91127, Palaiseau, France

(Received 8 March 2019; published 29 May 2019)

Quantum memories are a crucial element toward efficient quantum protocols. In the continuous variables domain, such memories need to provide high fidelity with an efficiency set to one. Moreover, one needs to store complex quantum states exhibiting negative Wigner functions after storage. We report the storage of single- and two-photon Fock states in an all-optical quantum memory. The Wigner functions of these states show negativity after a storage time of several hundred nanoseconds. This is, to our knowledge, the first demonstration of the storage in the optical domain of non-Gaussian states with more than one photon, captured from an external source and characterized with homodyne detection.

DOI: 10.1103/PhysRevLett.122.210501

Introduction.—A main bottleneck toward large-scale quantum-optics protocols concerns the ability to provide simultaneously several resources issued from nondeterministic protocols. Quantitatively, the synchronization of M heralded resources will be increased [1] (in the limit of low success rate) by a factor N^{M-1} with the use of $M-1$ quantum memories, each being able to wait for a maximum of N trials of its corresponding heralding source. This could permit experiments that are unrealistic to date. In this context, efficient quantum memories are an essential feature for the implementation of sophisticated operations. Over the last decade, numerous memories have been realized [2–4] in order to store quantum states using vapor cells [5], cold atoms [6–9], and crystals [10–13]. Those memories can provide long storage times (in the ms scale) but usually exhibit relatively low efficiencies. The concept of efficiency has a meaning for discrete variables protocols, when one can discard undetected events. The efficiency then quantifies the contribution of the memory to the detection probability [3]. When considering hybrid quantum protocols, with the use of continuous variables, the states are usually measured with homodyne or heterodyne detections. Unlike the discrete variables case, the measurement of field quadratures always leads to a result, regardless of the presence of photons in the observed optical mode: there is no "lost modes" in that case, and the efficiency has to be taken as one. Failed extractions have to be considered as vacuum, leading to a substantial drop of the fidelity. For that reason, most quantum memories developed so far are not suitable for continuous variables.

This ability to never lose any event is a main asset of continuous variable schemes and could allow the implementation of really efficient iterative protocols for the generation of new kind of optical quantum states [14–16]. For instance, it has been recently proved [17] that Gottesman-Kitaev-Preskill states [18] can be generated deterministically from optical Schrödinger cat states. Besides the need of efficient cat state sources [19–25], quantum memories are a central device in such iterative protocols, in order to capture and store a state produced at some generation stage, and to deliver it when required. When used with a nondeterministic protocol like the cat breeding scheme, a quantum memory can increase the success rate by several orders of magnitude [15], opening new perspectives in quantum optics.

In this context, the development of high-performance quantum memories is of major importance. Continuous variables quantum protocols rely on non-Gaussian states containing more than one photon [26–31], and a main asset of optical cavity-based quantum memories is their potentiality to store such states with high fidelity [32,33]. A key parameter of the generation of non-Gaussian states is the negativity of their Wigner functions (defined as their minimal value), which can be used as a quantitative witness of nonclassicality. Thus, the negativity of the stored states is an important parameter for characterizing quantum memories. In this Letter, we experimentally demonstrate the quantum storage, in an optical cavity, of Fock states up to the two-photon level, captured from an external source, delivered on demand, and exhibiting negative Wigner functions after dozens of round trips.

An optical quantum memory for hybrid protocols.—A scheme of the quantum memory is represented in Fig. 1: it consists in a cavity with a thin film polarizing beam splitter (PBS), represented as a cube in Fig. 1. A Pockels cell placed inside the cavity allows to switch the polarization of the light. Typically, a light pulse enters into the cavity with a horizontal polarization, and the Pockels cell allows to

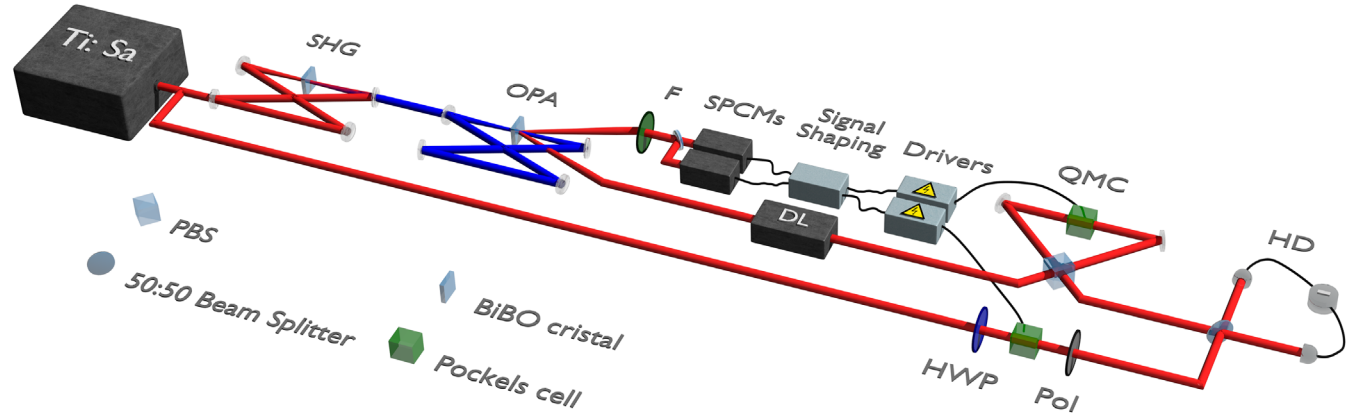

FIG. 1. Scheme of the setup. QMC, quantum memory cavity; F, spectral and spatial filters; DL, delay line; PBS, polarizing beam splitter; HWP, half-wave plate; Pol, polarizer.

rotate this polarization to vertical so that the pulse is then reflected by the PBS, and thus stored in the cavity. To extract the light, one just has to turn the polarization back to horizontal. The light can thus be delayed by an arbitrary number of round trips, with a synchronization that is warranted as the length of the cavity (3.9 m) matches the repetition rate of the laser (76 MHz).

Such kind of protocols have already been realized in the discrete regime [1,34,35]. In this regime, an issue could appear when the polarization degree of freedom is used to store the light, as such cavities cannot store information encoded in polarization. In the continuous variables domain, the information can be encoded using the quadratures degree of freedom, and the polarization is no longer matter of interest for information encoding. However, with continuous variables, no measurement can be ruled out: the efficiency of a quantum memory thus has to be taken as unity, and the different losses will reduce the fidelity of the output states.

Experimental setup.—A scheme of the experimental setup is shown in Fig. 1. Pulses from a Ti:sapphire laser with a central wavelength of 850 nm (temporal length 2.6 ps, repetition rate 76 MHz) are frequency doubled using a ∼3.9 m-long bow-tie second-harmonic-generation cavity with a type I BiB_3O_6 crystal [36,37]. The cavity, of finesse 60, allows to enhance the nonlinear effect, leading to a conversion efficiency of 70%. The output pulses at 425 nm are sent to another ∼3.9 m-long bow-tie cavity of finesse ≃80, namely the optical parametric amplification (OPA) cavity. The intracavity peak power reaches 40 kW. A second type I BiB_3O_6 crystal placed inside the OPA cavity allows to produce pairs of photons by noncolinear spontaneous parametric down-conversion (SPDC) [37].

As the phase matching of SPDC is broadband, the heralding part of the photon pairs, in the signal beam, is first spectrally and spatially filtered by the use of a single-mode fiber and a grating combined with a slit. The filtered photons are probabilistically separated by a beam splitter followed by two single-photon counting modules (Perkin Elmer SPCM-AQR-13) in order to detect the generation of single- and two-photon Fock states.

To account for the delay of the electronics (∼200 ns), the heralded state in the idler beam is sent through an optical delay line consisting in an open 4.8 m long cavity made of three mirrors [37]. The high transmission of this delay line constitutes a main asset of our setup compared to previous implementations of quantum memories based on optical cavities [1,34,35], where optical fibers were used in the delay path and induced higher insertion losses. The H-polarized Fock state is then transmitted by the PBS of the quantum memory and enters into the cavity. A 14 ns high-voltage pulse is applied to the Pockels cell in order to turn the polarization of the light pulse to vertical, and the Fock state is then stored inside the cavity. After a given number of round trips, the quantum state is extracted out of the cavity by rotating again its polarization. The extracted state is sent to a homodyne detection, together with the local oscillator pulse delivered by a second Pockels cell (see Fig. 1), in order to be characterized. The pulse from the local oscillator is sent to the homodyne detection only when a quantum state is extracted from the quantum memory. The few MHz bandwidth of the detection system is therefore compatible with the required analysis rates. The overall efficiency η of the homodyne detection is of $\eta_{\mathrm{HD}} = \eta_{\mathrm{PD}}\eta_{\mathrm{C}} = 77 \pm 3\%$ (where $\eta_{\mathrm{PD}} = 94 \pm 2\%$ is the quantum efficiency of the photodiodes, and $\eta_{\mathrm{C}} = \mathrm{C}^2 = 81 \pm 1\%$ is the mode-matching efficiency, with C the contrast measured between the idler beam and the local oscillator [38,39]).

As mentioned in the introduction, the probability to synchronize two quantum states depends on the number of round trips allowed in the cavity. The losses per round trip of the cavity are estimated to be 0.6%, leading to a theoretical lifetime of a single photon of $\tau = 2.2\ \mu$s (defined as $\mathcal{F} = \mathcal{F}_0 e^{-t/\tau}$, where $\mathcal{F}_0$ denotes the initial fidelity of the state [40]). The initial fidelity of the Fock

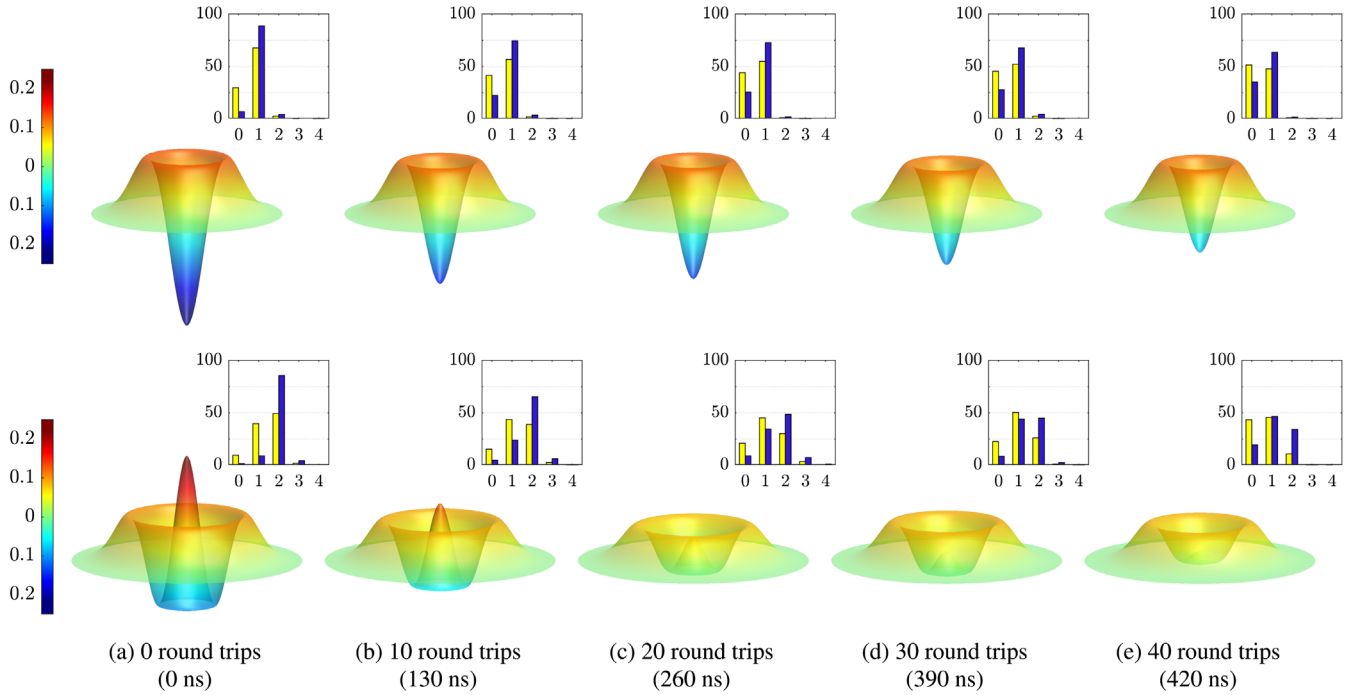

FIG. 2. Wigner function of the single-photon (top) and two-photon state (bottom) after different storage round trips: from 0 (a) to 40 (e) round trips. The Wigner functions are corrected from a 77% detection efficiency. Inset: diagonal elements of the density matrices without (light yellow) and with (dark blue) correction of the detection efficiency.

states (without storage) is another key parameter of the setup: the quality of the single-photon (two-photon) states reaches $91 \pm 4\%$ ($85 \pm 6\%$) after correction from the detection efficiency η, along with a production rate of 150–250 kHz (~200 Hz) [37].

Results and discussion.—To characterize the quantum memory, homodyne tomographies of the single-photon and two-photon states have been realized for different numbers of round trips inside the cavity. For a given number of round trips, 50 000 and 10 000 data points have been acquired for respectively the single-photon and two-photon measurements. As the Fock states are phase invariant, the phase of the homodyne detection was not measured. Once data are acquired, the density matrix and the Wigner function of the stored states, represented in Fig. 2, are reconstructed using a maximum likelihood technique [42] with correction of the detection efficiency η. The diagonal elements of the density matrices with and without correction of the efficiency are also shown in the insets of Fig. 2. As they increase with the number of round trips, the effect

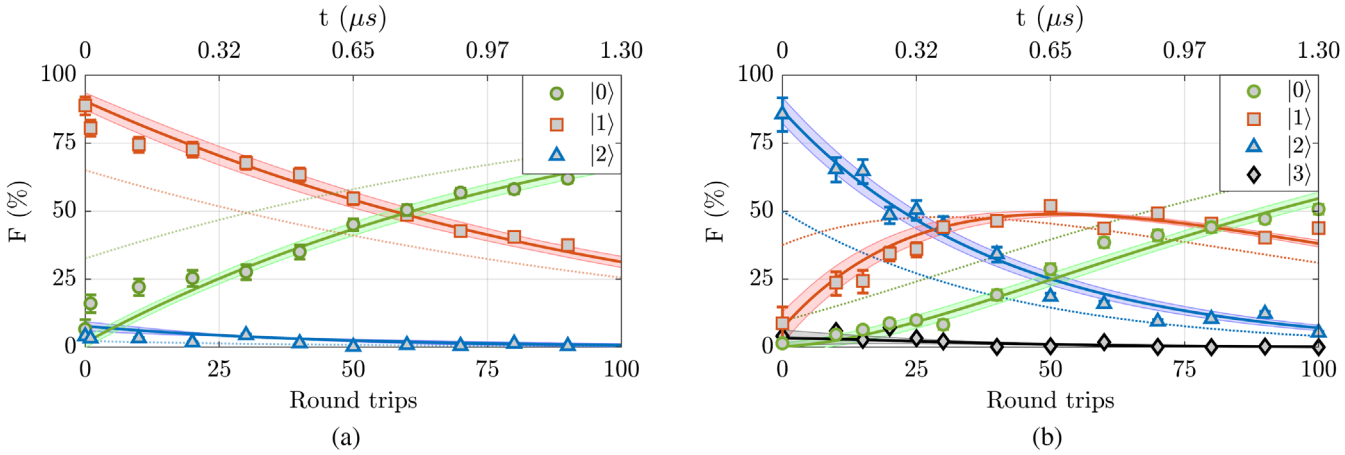

FIG. 3. Evolution of the diagonal elements of the density matrix of the stored state for the single-photon (a) and two-photon Fock state (b), as a function of the number of round trips (bottom axis) and of the storage time (top axis). The colored bands around the fits account for the uncertainty on the detection efficiency. The dotted curves represent the results without any correction from detection efficiency.

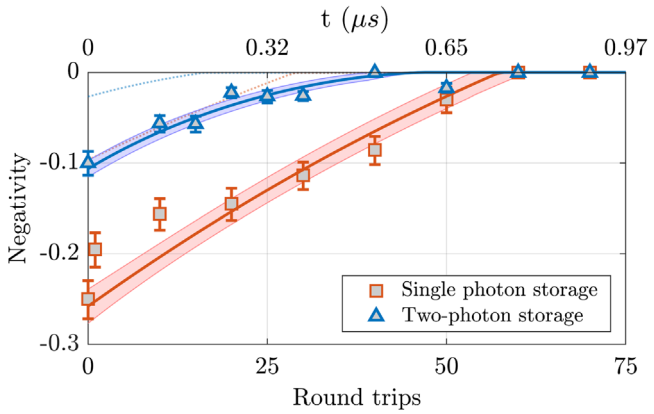

FIG. 4. Evolution of the negativity as a function of the number of round trips (bottom axis) and of the storage time (top axis). The colored bands around the fits account for the uncertainty on the detection efficiency. The dotted curves represent the results without any correction from detection efficiency.

of losses in the quantum memory reduces the fidelity of the stored states.

The values of the diagonal elements of the density matrix (corrected from the detection efficiency), which are the fidelities $\mathcal{F}_{|n\rangle} = \langle n|\rho|n\rangle$ of the stored state ρ with the Fock state $|n\rangle$, are represented in Fig. 3 for the single-photon Fock states (Fig. 3(a): red squares) and the two-photon Fock state (Fig. 3(b): blue triangles) as a function of the number of round trips of storage. The lifetimes are estimated to be of 1.44 and 0.51 μs for the single-photon and the two-photon states. Such a difference is explained by the quadratic effect of the losses on the two-photon states. As it reveals the nonclassicality of quantum states, the negativity of the Wigner function is a more relevant criteria than the lifetime for the characterization of memories in the continuous variable domain. The negativity of the reconstructed Wigner functions is directly plotted on Fig. 4. Starting at -0.25 ± 0.02 for the single-photon and -0.10 ± 0.02 for the two-photon state, the negativity is maintained over 50 round trips for both states. In both Figs. 3 and 4, error bars are deduced from the uncertainty on the detection efficiency η, which is the major error source in this experiment.

In order to evaluate the losses of the cavity, the evolution of the density matrix was fitted using the equation developed in Ref. [43]

$$\langle n|\hat{\rho}_N|n\rangle = (1-p)^{Nn} \sum_{i=0}^{\infty} \binom{n+i}{n} [1-(1-p)^N]^i \times \langle n+i|\hat{\rho}_0|n+i\rangle, \quad (1)$$

where p is the losses per round trip of the cavity and ρ_N is the density matrix of the states after N round trips of storage. The fits of the data in Fig. 3 show a good agreement with experimental data points. The losses per round trip can be extracted from the fits and are estimated to be of 1.0% for the single-photon and 1.3% for the two-photon experiment, exhibiting a slight decrease for the two-photon states. Such a difference could be explained by a longer acquisition time for the two-photon states, making the results more sensitive to experimental fluctuations. The losses per round trip do not only include the optical losses of the cavity, but also the evolution for the spatial mode of the quantum state inside the cavity as well as temporal mismatch between the cavity length and the repetition rate of the laser, leading to temporal and spatial mismatches between the local oscillator and the quantum state. The optical losses per round trip are estimated to be of 0.6%, which is close to the experimental values, showing a good control of the spatiotemporal mode of the stored quantum states.

The fits allow the determination of the negativities for each number of round trips of storage. For the single photons, this negativity starts at -0.26 ± 0.03, and the Wigner functions exhibit negativity after 57 ± 4 round trips of storage, corresponding to a 0.75 ± 0.05 μs storage time with preservation of this nonclassical feature. For the two-photon states, the Wigner functions remain negative until 46 ± 6 round trips, leading to a storage time of 0.61 ± 0.08 μs.

If one considers, for instance, a storage time of 20 round trips in the cavity, the fidelity of the stored single photon [Fig. 3(a)] is $73 \pm 3\%$. When compared to the fidelity of 91% of the initial state, this corresponds to losses of about only 20% from the memory: this is among the best values ever reported for quantum memories, and this performance includes the optical mode distortions that degrades the matching with the local oscillator at the homodyne detection. At the same time, as mentioned in the introduction, the success rate for the synchronization of $M+1$ resources would increase as 20^M, what would therefore represent a main technological breakthrough for quantum optics.

In conclusion, we have studied the storage of single- and two-photon Fock states in an all-optical cavity, reporting what is, to our knowledge, the first storage in the optical domain of a non-Gaussian state with more than one photon. The stored quantum states show negative Wigner functions until 57 ± 4 and 46 ± 6 round trips for single- and two-photon states, respectively, which correspond to a storage time of, respectively, 0.75 ± 0.05 and 0.61 ± 0.08 μs. Such cavities pave the way toward the synchronization of optical quantum states, which is a cornerstone in the direction of quantum information protocols.

The authors acknowledge support from the Région Ile de France DIM NANO-K for the HAQI project and from the Agence Nationale de la Recherche for the SPOCQ project (Grant No. ANR-14-CE32-019).

[1] F. Kaneda, F. Xu, J. Chapman, and P. G. Kwiat, Optica **4**, 1034 (2017).
[2] A. I. Lvovsky, B. C. Sanders, and W. Tittel, Nat. Photonics **3**, 706 (2009).

[3] C. Simon *et al.*, Eur. Phys. J. D **58**, 1 (2010).
[4] F. Bussières, N. Sangouard, M. Afzelius, H. de Riedmatten, C. Simon, and W. Tittel, J. Mod. Opt. **60**, 1519 (2013).
[5] K. F. Reim, P. Michelberger, K. C. Lee, J. Nunn, N. K. Langford, and I. A. Walmsley, Phys. Rev. Lett. **107**, 053603 (2011).
[6] E. Bimbard, R. Boddeda, N. Vitrant, A. Grankin, V. Parigi, J. Stanojevic, A. Ourjoumtsev, and P. Grangier, Phys. Rev. Lett. **112**, 033601 (2014).
[7] V. Parigi, V. D'Ambrosio, C. Arnold, L. Marrucci, F. Sciarrino, and J. Laurat, Nat. Commun. **6**, 7706 (2015).
[8] P. Vernaz-Gris, K. Huang, M. Cao, A. S. Sheremet, and J. Laurat, Nat. Commun. **9**, 363 (2018).
[9] D. Dong-Sheng, Z. Wei, Z. Zhi-Yuan, S. Shuai, S. Bao-Sen, and G. Guang-Can, Nat. Photonics **9**, 332 (2015).
[10] P. Jobez, C. Laplane, N. Timoney, N. Gisin, A. Ferrier, P. Goldner, and M. Afzelius, Phys. Rev. Lett. **114**, 230502 (2015).
[11] E. Saglamyurek, J. Jin, V. B. Verma, M. D. Shaw, F. Marsili, S. W. Nam, D. Oblak, and W. Tittel, Nat. Photonics **9**, 83 (2015).
[12] M. P. Hedges, J. J. Longdell, Y. Li, and M. J. Sellars, Nature (London) **465**, 1052 (2010).
[13] M. Sabooni, Q. Li, S. Kröll, and L. Rippe, Phys. Rev. Lett. **110**, 133604 (2013).
[14] J. Etesse, B. Kanseri, and R. Tualle-Brouri, Opt. Express **22**, 30357 (2014).
[15] J. Etesse, R. Blandino, B. Kanseri, and R. Tualle-Brouri, New J. Phys. **16**, 053001 (2014).
[16] H. M. Vasconcelos, L. Sanz, and S. Glancy, Opt. Lett. **35**, 3261 (2010).
[17] D. J. Weigand and B. M. Terhal, Phys. Rev. A **97**, 022341 (2018).
[18] D. Gottesman, A. Kitaev, and J. Preskill, Phys. Rev. A **64**, 012310 (2001).
[19] A. Ourjoumtsev, R. Tualle-Brouri, J. Laurat, and P. Grangier, Science **312**, 83 (2006).
[20] A. Ourjoumtsev, H. Jeong, R. Tualle-Brouri, and P. Grangier, Nature (London) **448**, 784 (2007).
[21] S. Deléglise, I. Dotsenko, C. Sayrin, J. Bernu, M. Brune, J.-M. Raimond, and S. Haroche, Nature (London) **455**, 510 (2008).
[22] T. Gerrits, S. Glancy, T. S. Clement, B. Calkins, A. E. Lita, A. J. Miller, A. L. Migdall, S. W. Nam, R. P. Mirin, and E. Knill, Phys. Rev. A **82**, 031802(R) (2010).
[23] J. Etesse, M. Bouillard, B. Kanseri, and R. Tualle-Brouri, Phys. Rev. Lett. **114**, 193602 (2015).
[24] K. Huang, H. L. Jeannic, J. Ruaudel, V. Verma, M. Shaw, F. Marsili, S. Nam, E. Wu, H. Zeng, Y.-C. Jeong, R. Filip, O. Morin, and J. Laurat, Phys. Rev. Lett. **115**, 023602 (2015).
[25] D. V. Sychev, A. E. Ulanov, A. A. Pushkina, M. W. Richards, I. A. Fedorov, and A. I. Lvovsky, Nat. Photonics **11**, 379 (2017).
[26] H. Jeong and M. S. Kim, Phys. Rev. A **65**, 042305 (2002).
[27] S. Lloyd and S. L. Braunstein, Phys. Rev. Lett. **82**, 1784 (1999).
[28] T. C. Ralph, A. Gilchrist, G. J. Milburn, W. J. Munro, and S. Glancy, Phys. Rev. A **68**, 042319 (2003).
[29] A. P. Lund, T. C. Ralph, and H. L. Haselgrove, Phys. Rev. Lett. **100**, 030503 (2008).
[30] S.-W. Lee and H. Jeong, Phys. Rev. A **87**, 022326 (2013).
[31] C. Silberhorn, T. C. Ralph, N. Lütkenhaus, and G. Leuchs, Phys. Rev. Lett. **89**, 167901 (2002).
[32] J.-i. Yoshikawa, K. Makino, S. Kurata, P. van Loock, and A. Furusawa, Phys. Rev. X **3**, 041028 (2013).
[33] K. Makino, Y. Hashimoto, J. i. Yoshikawa, H. Ohdan, T. Toyama, P. van Loock, and A. Furusawa, Sci. Adv. **2**, e1501772 (2016).
[34] T. B. Pittman and J. D. Franson, Phys. Rev. A **66**, 062302 (2002).
[35] F. Kaneda, B. G. Christensen, J. J. Wong, H. S. Park, K. T. McCusker, and P. G. Kwiat, Optica **2**, 1010 (2015).
[36] B. Kanseri, M. Bouillard, and R. Tualle-Brouri, Opt. Commun. **380**, 148 (2016).
[37] M. Bouillard, G. Boucher, J. F. Ortas, B. Kanseri, and R. Tualle-Brouri, Opt. Express **27**, 3113 (2019).
[38] U. Leonhardt, *Measuring the Quantum State of Light* (Cambridge University Press, Cambridge, England, 1997), Vol. 22.
[39] A. I. Lvovsky, H. Hansen, T. Aichele, O. Benson, J. Mlynek, and S. Schiller, Phys. Rev. Lett. **87**, 050402 (2001).
[40] $\mathcal{F} = \mathrm{tr}(\rho|\psi\rangle\langle\psi|)$ where $|\psi\rangle$ is the reference state and ρ the experimental density matrix [41].
[41] R. Jozsa, J. Mod. Opt. **41**, 2315 (1994).
[42] A. I. Lvovsky, J. Opt. B **6**, S556 (2004).
[43] T. Kiss, U. Herzog, and U. Leonhardt, Phys. Rev. A **52**, 2433 (1995).